Since January 2020 Elsevier has created a COVID-19 resource centre with free information in English and Mandarin on the novel coronavirus COVID-19. The COVID-19 resource centre is hosted on Elsevier Connect, the company's public news and information website.

Talanta 239 (2022) 123113

Contents lists available at ScienceDirect

Talanta

journal homepage: www.elsevier.com/locate/talanta

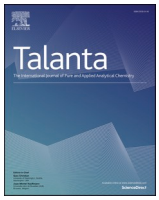

Antibody mounting capability of 1D/2D carbonaceous nanomaterials toward rapid-specific detection of SARS-CoV-2

Seyyed Alireza Hashemi [a,1], Sonia Bahrani [b,1], Seyyed Mojtaba Mousavi [c,1], Navid Omidifar [d,e,*], Nader Ghaleh Golab Behbahan [f], Mohammad Arjmand [a,**], Seeram Ramakrishna [g,***], Ayrat M. Dimiev [h], Kamran Bagheri Lankarani [b], Mohsen Moghadami [i], Mohammad Firoozsani [j]

[a] Nanomaterials and Polymer Nanocomposites Laboratory, School of Engineering, University of British Columbia, Kelowna, BC, V1V 1V7, Canada
[b] Health Policy Research Center, Health Institute, Shiraz University of Medica Sciences, Shiraz, Iran
[c] Department of Chemical Engineering, National Taiwan University of Science and Technology, Taiwan
[d] Department of Pathology, Medical School, Shiraz University of Medical Sciences, Shiraz, Iran
[e] Clinical Education Research Center, Shiraz University of Medical Sciences, Shiraz, Iran
[f] Razi Vaccine and Serum Research Institute, Agricultural Research, Education and Extension Organization (AREEO) Shiraz Branch, Shiraz, Iran
[g] Department of Mechanical Engineering, Center for Nanofibers and Nanotechnology, National University of Singapore, Singapore
[h] Laboratory for Advanced Carbon Nanomaterials, Kazan Federal University, Kremlyovskaya st., 18, Kazan, Russian Federation
[i] Non-Communicable Diseases Research Center, Shiraz University of Medical Sciences, Shiraz, Iran
[j] Member of Board of Trustees, Zand Institute of Higher Education, Shiraz, Iran

ARTICLE INFO

Keywords:
Graphene
Carbon nanotube
SARS-CoV-2
Covid-19
Electrochemical detection

ABSTRACT

Carbonaceous immunosensors are ideal nanoplatforms for developing rapid, precise, and ultra-specific diagnostic kits capable of early detection of viral infectious illnesses such as COVID-19. However, developing a proper carbonic immunosensor requires stepwise protocols to find optimum operating conditions to minimize drawbacks. Herein, for the first time and through a stepwise protocol, activation, and monoclonal IgG antibody mounting capability of multi-walled carbon nanotubes (MWCNTs) at two diverse outer diameters (ODs), viz., 20–30 nm and 50–80 nm, and graphene deriv atives (graphene oxide (GO) and reduced graphene oxide (rGO)) were examined and compared with each other toward finding the prime carbonaceous nanomaterial(s) for maximized antibody loading efficiency along with an ideal detection limit (DL) and sensitivity. Next, the effect of common amplifying agents, i.e., Au nanostars (Au NSs) and Ag nanowires (Ag NWs), on the total performance of the best carbonaceous structure was carefully assessed, and the responsible detection mechanism is investigated in detail. Next, the developed carbonaceous immunosensors were assessed via voltammetric and impedance assays, and their performances toward specific detection of SARS-CoV-2 antigen through immunoreaction were examined in detail. The study's outcome showed the superior performance of conjugated rGO-based immunosensor with Au NSs toward specific and quick (1 min) detection of SARS-CoV-2 antigen in biological fluids compared with other 1D/2D carbonaceous nanomaterials.

1. Introduction

The widespread of viral infectious diseases and their subsequent mortalities raised an urgent requirement for developing a diagnostic kit capable of rapid and specific detection of viruses in diverse biological specimens. Among these viral infectious illnesses, the outbreak of COVID-19 can be mentioned, which caused a severe threat for humanity through an ultra-fast person-to-person transmission that cannot be furtherly controlled via common time-consuming traditional detection approaches, i.e., RT-PCR and ELISA [1,2].

The main point in pausing rapid spreadable viral pandemics passes through the development of rigorous isolation strategies via the design/

* Corresponding author. Department of Pathology, Medical School, Shiraz University of Medical Sciences, Shiraz, Iran.
** Corresponding author.
*** Corresponding author.
E-mail addresses: omidifarn@sums.ac.ir (N. Omidifar), mohammad.arjmand@ubc.ca (M. Arjmand), seeram@nus.edu.sg (S. Ramakrishna).
[1] These authors have equal contribution in the preparation of this manuscript and accomplishing experimental works.

https://doi.org/10.1016/j.talanta.2021.123113
Received 5 August 2021; Received in revised form 17 October 2021; Accepted 26 November 2021
Available online 29 November 2021
0039-9140/

development of rapid, specific/sensitive kits capable of detecting suspected people even in the silent stage of an illness [3,4]. Despite the urgent requirement for a rapid sensor and/or diagnostic kit, healthcare authorities still using traditional detection approaches, viz., ELISA and RT-PCR, that suffering from serious demerits, including sophisticated laboratory instruments, isolation of viral particles, extraction of viral RNA, expert manpower, high rate of false-negative outcomes and time-demanding protocols that are not matched with the rapid spread speed of SARS-CoV-2 and wise isolation policy for stopping the pandemic [5]; hence, it is vital to consider alternative approaches to deeply address this demand for future viral pandemics.

Novel biosensors and/or nanosensors can address this demand and be considered as a capable alternative instead of traditional detection approaches owing to their tunable features, marvelous sensitivity/specificity, and above all, rapid detection of pathogenic viruses in less than 1 min [6]. Among developed sensors, electrochemical biosensors/nanosensors are known as fantastic analytical tools compared to their counterparts due to their self-control, low cost, and excellent portability [7]. Correspondingly, among such marvelous sensors, immunosensors created a new pathway toward rapid, sensitive, and specific detection of target biological markers due to the combination of specificity of a bio-immunoreaction with sensitive electrochemical detectors based on nanomaterials [8,9]. These capable tools, viz., immunosensors, are potential platforms for detecting the specific biological binding between an antibody and a target antigen by forming a highly stable biochemical complex via immunoreaction [10,11]. Moreover, a capable biosensor had better to be accompanied by a vast range of essential characteristics, among which sensitivity, specificity, selectivity, accessibility, user-friendliness, rapid assessment speed, simplicity of equipment, and ease of deliverability for the end-user can be mentioned.

Additionally, graphene oxide (GO) is a proper 2D nanoflake for nanosensor applications owing to its transducer property, ease of production, massive specific surface area, and ideal sensitivity [12]. Accordingly, due to abundant hydrophilic polar moieties and active oxygen-based functional groups on the surface of GO flakes, it could be homogeneously dispersed in aqueous media and generate highly uniform complexes [13]. Likewise, these active functional groups shed light on new opportunities in biology for perfect binding with functional linker groups and/or antibodies because of their superior hydrophilic nature. More importantly, custom functionalization of GO's surface provides great merit for decorating its surface with selected bio/chemical compounds through either covalent or non-covalent bindings [14,15]. However, GO is an insulator nanoflake, and it is essential to promote its conductivity through reduction processes to make it suitable for bio-applications [16,17]. What is more, the specification of sensing interfaces as core parts of label-free immunosensors holds a great level of importance. Therefore, these interfaces had better be accompanied by a wide active surface area and excellent electrical conductivity of a proper nanostructure to improve the quality of the output signal [18–20]. Hence, carbonaceous nanomaterials such as graphene derivatives and carbon nanotubes (CNTs) could be considered as potential candidates to address this crucial demand because of their extraordinary properties [17,21–24].

In this matter, graphene by-products and carbon nanotubes (CNTs) have been widely used to develop practical immunosensors due to their wide active surface area, and unique electrical, physical, and chemical properties, make them ideal candidates for mounting antibodies with high efficiency [17,21,22]. Correspondingly, several attempts were conducted to use graphene to develop immunosensors for detecting SARS-CoV-2 antigen within biological samples. For instance, a field-effect graphene-based immunosensor based on the monoclonal IgG antibody of SARS-CoV-2's spike protein was developed, which managed to detect the SARS-CoV-2 antigen in biological fluids with a detection limit of 2.42×10^2 copies.mL^{-1} [25]. In another attempt, Torrente-Rodríguez et al. [26] developed a multiplexed graphene-based diagnostic platform capable of simultaneous detection of several biomarkers, including IgG/IgM antibodies, nucleocapsid protein, and C-reactive protein, as a sign of inflammatory toward rapid and precise detection of SARS-CoV-2 through a multiplexed manner within biological/non-biological media. Obtained outcomes clearly highlighted a glaring requirement for developing novel, rapid and specific biosensors instead of traditional approaches, viz., ELISA, and RT-PCR, capable of detecting pathogenic viruses in diverse biological specimens.

In addition, precious metallic nanomaterials based on Au, Pt, Ag, and Pd along with their alloys provided a great opportunity for improving the performance of *in-vivo* or *in-vitro* biosensors due to their superior chemical, physical and electrochemical properties along with their outstanding biocompatibility [27]. Au nanoparticles provide some exciting pros and can meet numerous vital criteria, e.g., perfect chemical stability, surface-to-volume ratio, vast working potential range, ideal catalytic behavior, and outstanding biocompatibility, make them ideal for conjunction with immunosensors or biosensors [28]. In Table 1, a list of the recently developed sensor for rapid, sensitive, and specific detection of SARS-CoV-2 in biological samples is tabulated.

What is more, a stepwise protocol has not been designed/developed to evaluate the dimension/feature dependence of carbonaceous nanomaterials toward fabrication of highly sensitive/specific immunosensor for early detection of pathogenic viruses within diverse aquatic media. Herein, for the first time, we have developed a stepwise protocol toward designing and developing label-free 1D/2D carbonaceous immunosensors mounted with monoclonal IgG antibody against S1 part of S spike glycoprotein of SARS-CoV-2 toward early detection of SARS-CoV-2 antigen within biological/non-biological fluids. For this aim, first activation and antibody mounting capability of 1D (multi-walled carbon nanotube (MWCNT) with an outer diameter (OD) of 20–30 nm and 50–80 nm) and 2D (graphene oxide (GO) and reduced graphene oxide (rGO)) carbonaceous nanomaterials were assessed via electrochemical approaches, and their performances were compared with each other to find the optimum substrate for efficient loading of antibodies (Fig. 1). Thence, the optimum carbonaceous platform was conjugated with either Au nanostars (Au NSs) or Ag nanowires (Ag NWs) to check the effect of amplifiers on the final response of the immunosensor to the target antigen. Afterward, the selected optimum platform was assigned to diverse analyses, and their antigen detection mechanism/performance was assessed through stepwise rigorous electrochemical evaluations.

2. Results and discussions

2.1. Electrochemical assessment of 1D/2D carbonaceous nanomaterials

In this section, the electrochemical performance of 1D/2D carbonaceous nanomaterials, i.e., MWCNTs (at two diverse ODs), GO, and rGO, were assessed and compared with each other to find the most proper substrate for mounting monoclonal IgG antibody against S1 glycoprotein of SARS-CoV-2. To trace the efficiency of the prepared electrodes, comparative impedance and voltammetric measurements were carried out in the 5 mM $(Fe(CN)_6)^{4-}/(Fe(CN)_6)^{3-}$ redox couple. Fig. 2(a–d) illustrate the outcome of CV analyses for bare GCE and coated GCE with activated immunosensors based on MWCNT with OD of 20–30 nm (a), MWCNT with OD of 50–80 nm (b), GO (c) and rGO (d). Accordingly, the effect of MWCNT's outer diameter and reduction of GO on the NHS/EDC activation and antibody mounting capability of carbonaceous nanomaterials were assessed. In all of the selected carbonaceous nanomaterials, the height of anodic peaks (I_{pa}) was declined upon each stepwise modification, i.e., activation of the carbonaceous compound with NHS/EDC complex and subsequent loading of antibodies. Decline in the current response of carbonaceous nanomaterials after activation by NHS/EDC and attachment to antibodies vividly indicating the prosperous immobilization of antibodies on the surface of carbonaceous nanomaterials. This outcome can be elucidated via the shielding barrier of immunocomplexes on the surface of the modified electrode, which

Table 1
Summary of recently developed sensors toward the accurate detection of SARS-CoV-2.

Sensor Type	Sensor Configuration	Obtained Outcomes	Target(s)	Ref.
Electrochemical Immunosensor	Decorated Magnetic nanoparticles with IgG antibodies	Sensitivity: NR DL: 19 ng mL^{-1} (for S protein) 8 ng mL^{-1} (for N protein) Method: DPV	N protein and S spike glycoprotein of SARS-CoV-2	[29]
Electrochemical Nanosensor	Decorated graphene with 8H/EDC/NHS	Sensitivity: 0.0048 μA $(\mu g/mL)^{-1}.cm^{-2}$ DL: 1.68 × 10^{-22} μg mL^{-1} Method: DPV	SARS-CoV-2 virus and S spike glycoprotein	[6]
Electrochemical Elisa	Decorated graphene with 8H/EDC/NHS	Sensitivity: 2.14 μA$(\%V/V)^{-1}.cm^{-2}$ DL: 0.18 × 10^{-18} %V/V Method: DPV	Monoclonal antibody of SARS-CoV-2	[3]
Electrochemical Biosensor	Decorated FTO-Au with IgG antibodies	Sensitivity: NR DL: 90–120 fM Method: DPV	S spike glycoprotein of SARS-CoV-2	[30]
Field-Effect Transistor	modified graphene with IgG antibodies	Sensitivity: NR DL: 2.24 × 10^{2} copies. mL^{-1} Method: DPV	spike glycoprotein of SARS-CoV-2	[25]
Electrochemical Biosensor	Decorated GO with calixarene	Sensitivity: NR DL: 200 copies.mL^{-1} Method: DPV	RNA of SARS-CoV-2	[31]
Electrochemical Nanosensor	Modified graphene with 8H/β-CD/EDC/NHS	Sensitivity: 13.18 μA$(fg/mL)^{-1}.cm^{-2}$ (for SARS-CoV-2) 9.01 μA$(fg/mL)^{-1}.cm^{-2}$ (for H_1N_1) 20.06 μA$(fg/mL)^{-1}.cm^{-2}$ (for H_3N_2) DL: 0.1802 fg mL^{-1} (for SARS-CoV-2) 0.191 fg mL^{-1} (for H_1N_1) 0.298 fg mL^{-1} (for H_3N_2) Method: DPV	SARS-CoV-2, H_1N_1, and H_3N_2 viruses	[32]
Electrochemical Immunosensor	Modified MWCNT and graphene derivates with IgG antibodies	Sensitivity: rGO-NHS/EDC-AB: 451.21 μA$(fg/mL)^{-1}.cm^{-2}$ rGO-NHS/EDC-AB-Ag NWs: 311.17 μA$(fg/mL)^{-1}.cm^{-2}$ rGO-NHS/EDC-AB-Au NSs: 342.52 μA$(fg/mL)^{-1}.cm^{-2}$ DL: rGO-NHS/EDC-AB: 0.0011 fg mL^{-1} rGO-NHS/EDC-AB-Ag NWs: 0.0065 fg mL^{-1} rGO-NHS/EDC-AB-Au NSs: 0.0010 fg mL^{-1} Method: DPV	SARS-CoV-2 virus	Current work

Abbreviations: DL: detection limit, NR: not reported, N: nucleocapsid, EDC: 1-ethyl-3-(3-dimethylaminopropyl)carbodiimide, 8H: 8-hydroxyquinoline, NHS: N-hydroxysuccinimide, FTO: fluorine-doped tin oxide, DPV: differential pulse voltammetry, β-CD: β-Cyclodextrin, AB: antibody, NW: nanowire, and NS: nanostar.

obstructed the electron transfer rate of $(Fe(CN_6))^{3-/4-}$ redox couple. Besides, the anodic/cathodic peak potential is shifted toward positively/negatively charged regions that are accompanied by a distinguished peak separation after each modification step, indicating irreversible behaviour and limitation in the electron transfer rate of the as-developed configurations upon formation of immunocomplexes on the surface of 1D or 2D carbonaceous nanomaterials. However, the redox signals of $(Fe(CN)_6)^{3-/4}$ were remarked upon introducing Au NSs and Ag NWs to the immunosensor due to the inherent conductivity of Au NSs and Ag NWs, which facilitate the charge transfer rate in the solution [33]. In Table S2 and section 3 of the supporting information, further data regarding the effect of potential scan rate on the response of the immunosensor along with the effective electrocatalytic surface area of each developed carbonaceous compound can be seen.

In addition, further assessment of developed immunosensors was performed via EIS analysis. Impedance spectroscopy is a key technique to appraise the interfacial changes of the bare and modified working electrodes within the frequency range from 0.1 to 10^5 Hz [34]. Obtained data from the EIS analyses are in perfect accord with the results of CV analyses, which can vividly be seen in Fig. 3 parts (a) and (b). Revealed semicircle shapes in the Nyquist diagrams demonstrate the parallel combination of R_{ct} and C_{ϕ} resulting from the electrode impedance. The semicircle shape of the Nyquist plot depicts a limited kinetic process at higher frequencies and a diffusion-limited electron transfer process at lower frequency ranges. To obtain vital information regarding the electron transfer rate of the developed electrodes, R_{ct} values and other impedance data were approximated for bare GCE and modified electrode with immunosensor by fitting the outcome of the Nyquist graph with equivalent Randles circuit model. The electron transfer kinetic parameters, including R_s, R_{ct}, and C_{ϕ} are related to the kinetic of electrode-electrolyte interface processes. R_s exhibits the resistance of the

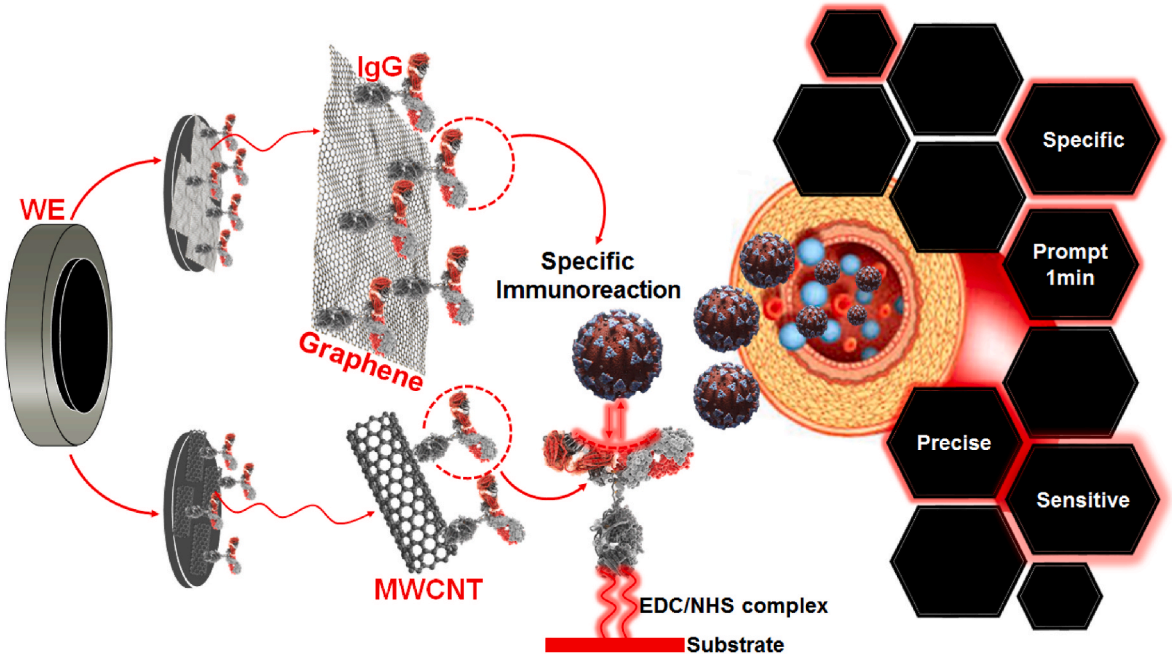

Fig. 1. Graphene-based compounds *vs.* CNT-based platforms toward developing rapid, specific, and sensitive immunosensors; WE: working electrode.

electrolyte solution, while the C_{ϕ} parameter is the pseudo-capacitance and known as a fundamental concept in the theoretical treatment of the adsorption process that describes the redox reaction of the surface-confined electroactive compounds. The extracted data regarding these parameters for considered configuration is tabulated in Table S3.

As clearly tabulated in Table S3, both MWCNTs with OD of 20–30 nm and 50–80 nm (Fig. 3 (a) (I) and (II)) exhibit a straightforward line with a tiny semicircle arc at a higher frequency which shows that the process is governed via the diffusion-limited electron-transfer process on the top active surface area of the modified electrode. The low impedance value of these films is due to the high conducting nature of MWCNTs at the electrode-electrolyte interfaces.

Besides, as can be seen in Fig. 3 (b) (I) and Table S3, the outcome of EIS analysis for coated GCE with GO showed an enlarged semicircle pattern at higher frequency ranges with a small interface impedance and a larger impedance value for GO-based immunosensor, which could be attributed to the presence of negative charges on the surface of GO sheets and electrostatic repulsion between negative charges of the oxygen-based functional groups on the surface of GO and the electroactive probe $(Fe(CN)_6)^{3-/4-}$. Accordingly, GO is a practical intermediate in electrocatalytic reactions owing to its strong adsorptive capability and precise electrical characteristics. In this matter, soar in the R_{ct} values after each modification step can be explicated via the intrinsic semiconductor nature of GO sheets coated on the top surface of the working electrode and the barrier effect of immunocomplexes on the surface of GCE. Additionally, reducing GO to rGO via chemical approaches considerably improved the capability of the developed immunosensor and provided more available NHS/EDC activated –COOH sites on the top surface of electrodes prior to antibody immobilization (Fig. 3 (b) (II)).

In addition, activation of carbonaceous nanomaterials with NHS/EDC complex and load of monoclonal IgG antibodies on their surfaces lead to the generation of a semicircle region in the Nyquist plots, arise from the boosted electron transfer resistance of the modified carbonaceous immunosensors. These outcomes clearly show the successful modification of selected carbonaceous compounds by NHS/EDC complex and linkage of antibodies on their surface via their activated functional groups. Likewise, linkage of antibodies to NHS/EDC modified carbonaceous compounds can significantly increase the final R_{ct} values due to the barrier effect of linked antibodies on the surface of modified electrodes.

Additionally, restoring the graphitic structure of graphene upon reduction of GO to rGO through chemical processes leads to higher electrical conductivity and enhances the electrocatalytic activity of the rGO compared with the GO. From EIS data (Fig. 3 (b) (I) and (II)), it can be seen that both GO and rGO representing better antibody loading capability compared with MWCNTs. In contrast, rGO exhibited a far stronger antibody loading rate than GO, making it ideal for developing efficient immunosensors. Obtained data are vividly in accord with the outcome of CV analyses, suggesting successful activation of carbonaceous nanomaterials with NHS/EDC complex and load of monoclonal IgG antibodies via generated activated functional groups on their surfaces. In this matter, electrode modification step could occur due to possible hydrogen bonding and attachment of antibodies to the surface of the carbonaceous substrate via NHS/EDC linkage, change in the situation of active functional groups upon adsorption process by each respective layer, deposition/attachment of nanomaterials on the surface of electrodes and soar in the film thickness. Further details regarding the antibody loading capability of carbonaceous compounds can be seen in section 3 of the supporting information and Table S3.

Based on the achieved data by CV and EIS analyses, rGO as a potential electroactive 2D carbonaceous flake considered as the optimum platform owing to its higher active surface area, higher porosity or surface inhomogeneity, fantastic antibody loading capability, and boosted electrocatalytic performance along with ideal electrical conductivity compared with its counterparts. Therefore, rGO is considered a base for developing immunosensors based on monoclonal IgG antibodies against S1 glycoprotein of SARS-CoV-2 toward accurate detection of betacoronaviruses in aquatic biological media. Additionally, the concentration (r) of immobilized antibodies on activated carbonaceous nanomaterials can be calculated by DPV method from the following equation [35]:

$$\Gamma = Q/nFA$$

In the above equation, the r as the overall amount of loaded monoclonal antibodies on the surface of MWCNT (20–30 nm)-NHS/EDC, MWCNT (50–80 nm)-NHS/EDC, GO-NHS/EDC, and rGO-NHS/EDC were measured to be 1.06×10^{-10}, 9.45×10^{-10}, 4.21×10^{-9} and

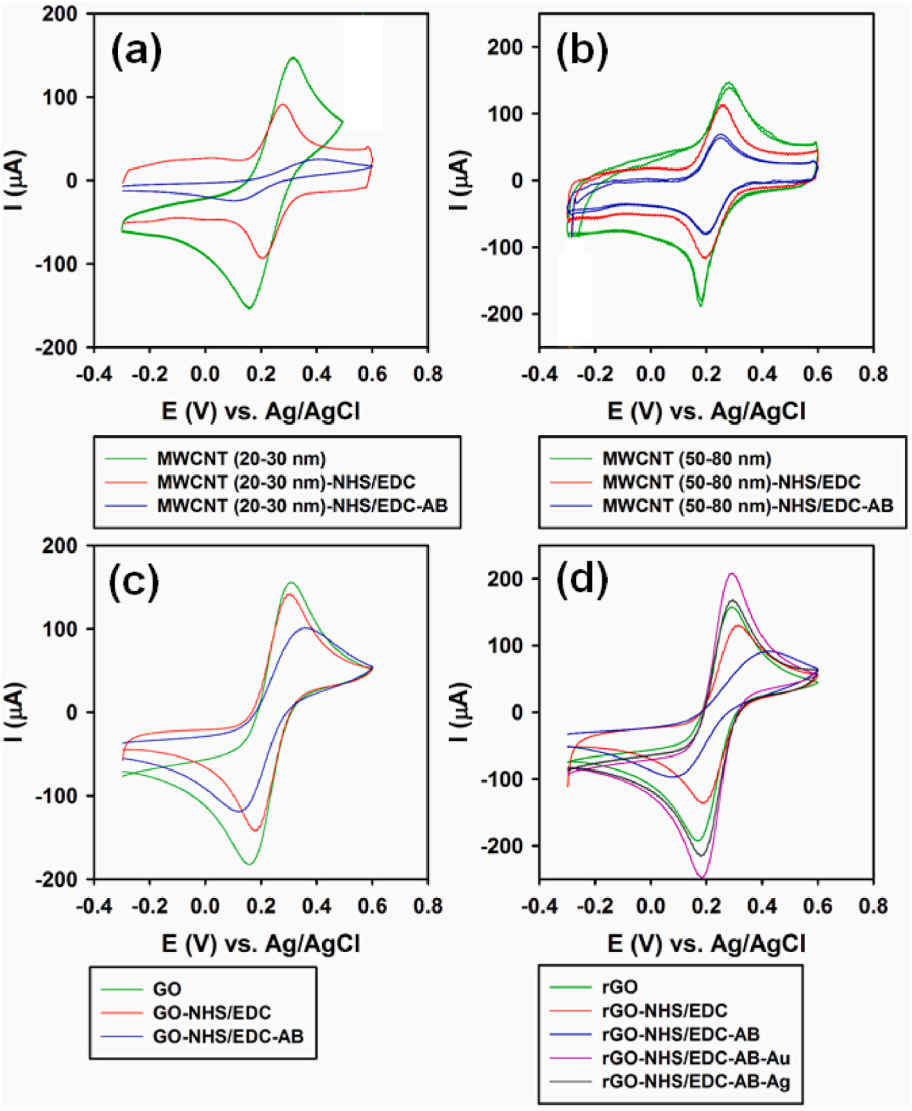

Fig. 2. CV analyses of (a) MWCNT with OD of 20–30 nm, (b) MWCNT with OD of 50–80 nm and (c) GO prior and after modification with NHS/EDC and NHS/EDC-antibody (AB); (d) CV analyses of rGO prior/after modification with NHS/EDC and NHS/EDC-AB along with conjunction with Ag NWs and Au NSs as capable amplifying agents.

6.33×10^{-9} mol cm^{-2}, respectively. According to the obtained data, 2D graphene derivatives, e.g., GO and rGO, presented far better antibody loading efficiency than 1D CNTs, which highlights the potential of graphene as a capable substrate for developing practical immunosensors. In Fig. 3 (c), a 3D view of employed carbonaceous structures can be seen.

2.2. Optimum carbonaceous immunosensor toward specific detection of SARS-CoV-2

After selecting rGO as the optimum carbonaceous compound due to its superior antibody mounting capability and vividly higher specific active surface area than its counterparts, the subsequent immunosensor based on rGO was applied to diverse analyses to assess its total electrochemical performance. Accordingly, the electrocatalytic performance of rGO-based immunosensors regarding the rapid detection of SARS-CoV-2 in biological/non-biological fluids was initially traced by the DPV technique in the PBS 0.01 M with pH 7.4, pulse amplitude of 25 mV, and width of the pulse of 50 ms.

In Fig. 4 (a), the voltammetric response of immunosensors based on diverse carbonaceous nanomaterials can be seen. As depicts, graphene-based flakes showed the best performance with higher intensity compared with CNT-based compounds. In this matter, at viral antigen's concentration of 0.02 fg mL^{-1}, reduction of GO to rGO increased the intensity by about 13.83%, while the increase in the outer diameter of MWCNTs from 20-30 nm to 50–80 nm increased the intensity of immunosensor of about 33.24%. According to the obtained outcomes, immobilization of monoclonal IgG antibodies with rGO nanoflakes can significantly improve the total response to SARS-CoV-2 antigen via DPV analyses, which further confirm previously obtained data regarding the better performance of rGO toward the development of efficient immunosensors.

Fig. 4 (b) parts (I) and (II) depict the current response of the optimum immunosensor based on rGO-NHS/EDC-AB toward detection of inactivated antigen of SARS-CoV-2 in PBS with pH 7.4. In this matter, the immunosensor responded to the antigen and generated a specific signal at a voltage position of about 0.031 V, which was subsequently soared upon a further increase in the concentration of SARS-CoV-2 antigen within the biological and/or non-biological fluids. More importantly, the immunosensor responded to the lowest concentration of viral antigen, viz., 19 times (10^{-19}) one to ten dilution of the stock solution of antigen with $10^{9.4}$ TCID50, and generated a unique specific signal in

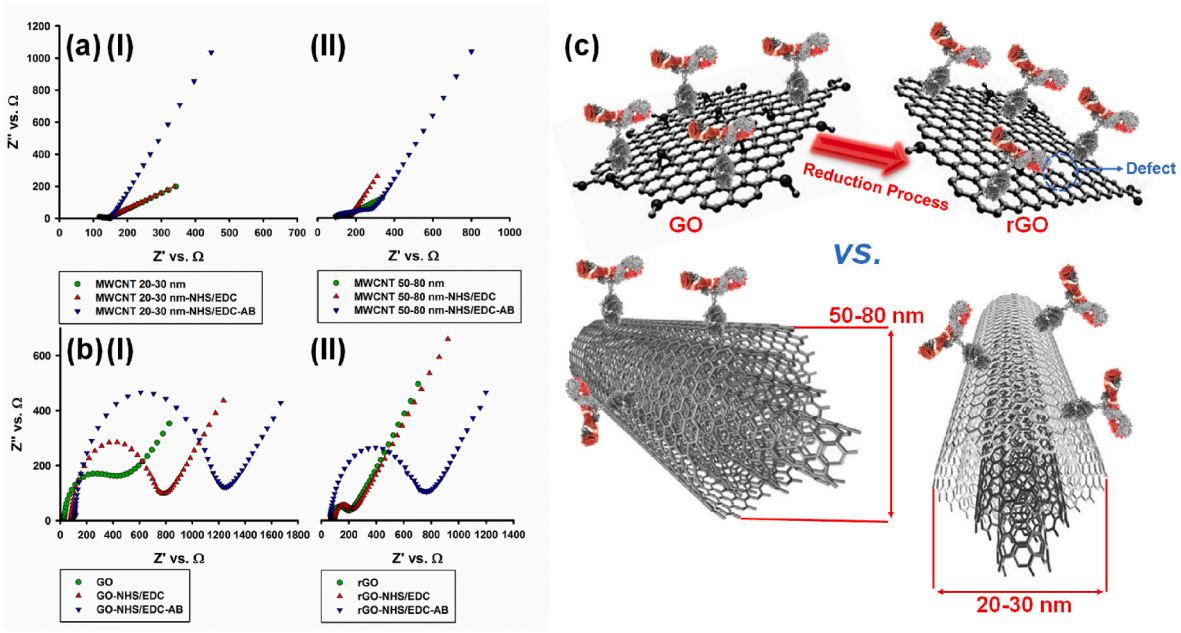

Fig. 3. (a) EIS parameters of (I) MWCNTs with OD of 20–30 nm and (II) MWCNTs with OD of 50–80 nm prior and after modification with NHS/EDC and NHS/EDC-antibody (AB) complexes, (b) EIS parameters of (I) GO and (II) rGO prior and after modification with NHS/EDC and NHS/EDC-AB complexes, and (c) antibody mounting capability of MWCNTs vs. graphene by-products.

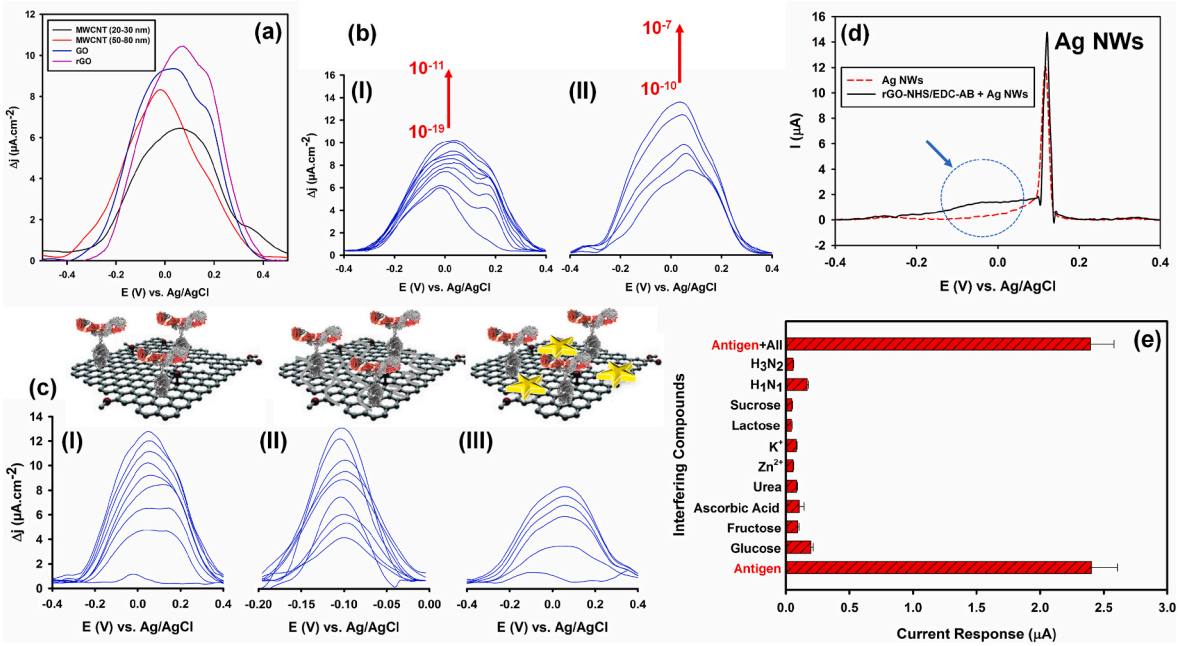

Fig. 4. (a) response of diverse carbonaceous nanomaterials to the immunosensor upon absorption of SARS-CoV-2 antigen through immunoreaction; (b) stepwise addition of standard stock of SARS-CoV-2 antigen with a primary stock of $10^{9.4}$ TCID50 to the PBS with pH 7.4 and subsequent response of the immunosensor at concentrations between (I) 10^{-19}-10^{-11} and (II) 10^{-10}-10^{-7}; (c) DPV response of immunosensor based on (I) rGO-NHS/EDC-AB, (II) rGO-NHS/EDC-AB + Ag NWs and (III) rGO-NHS/EDC-AB + Au NSs at variable concentrations of SARS-CoV-2 antigen in human blood plasma samples; (d) effect of Ag NWs on the current response of rGO-NHS/EDC-AB immunosensor, (e) effect of interfering compounds on the current signal/response of rGO-NHS/EDC-AB immunosensor in conjunction with Au NSs.

response to the immunoreaction between antibody and target antigen. This well-defined peak at a specific voltage position revealed the ideal capability of the immunosensor toward specific detection of SARS-CoV-2 antigen in aqueous biological samples and demonstrated the capability of the immunosensor toward ultra-specific detection of SARS-CoV-2 antigen.

To improve the sensitivity and detection limit of the developed sensor, the proposed platform was furtherly modified with two conductive metal-based nanomaterials, including Ag NWs and Au NSs. Correspondingly, a certain amount of carbonaceous immunosensors based on rGO nanoflakes were well-dispersed in a solution containing either Ag NWs or Au NSs. For further assessment of the modified electrode toward detecting viral antigen and gaining the analytical figures of merits, the respective calibration curve of the modified electrode with

carbonaceous immunosensor was also recorded within the human plasma sample as the aquatic biological medium. The calibration curves of viruses using diverse immunosensors were plotted, and their obtained outcomes are demonstrated in Table 2 and Figure S4. In Fig. 4 (c) (I), the quantitative analyses of SARS-CoV-2 in human blood plasma was carried out through the generation of diverse voltammetric patterns of SARS-CoV-2 through variating the concentration of virus in optimized conditions; the respective calibration curve of this graph is illustrated within Figure S4 (a). The calibration curve is achieved via plotting the concentration of standard viral suspension versus the height of generated signals in μA. As shown in Fig. 4 (c) (I) and Figure S4 (a), the appeared current signals were soared upon an increase in the concentration of viral antigen, which is due to the absorption of antigen on the surface of the immunosensor through direct immunoreaction between the monoclonal IgG antibody and target antigen.

The generated currents signal from the immunoreaction appeared at about 0.036 V and increased upon further stepwise addition of viral antigen to the electrolyte. These signals were furtherly confirmed the specific detection of antigen via the immunosensor owing to the well-affinity of the monoclonal IgG antibody against S1 glycoprotein of SARS-CoV-2 with its target antigen that absorbed the antigen via highly specific immunological interactions upon introduction of rGO-NHS/EDC-AB on the active surface area of the working electrode as a catalytic mediator. Correspondingly, the linear relationship between virus concentrations and generated current signals' intensity can be expressed as ΔJ ($\mu A.cm^{-2}$)=14.168 C ($fg\ mL^{-1}$)+0.0366 with R^2 of 0.9893, which exhibits a reasonable detection limit (DL, S/N=3)/sensitivity (m/A); a view of these outcomes is tabulated within Table 2 [36].

Furthermore, in Fig. 4 (c) (II) and (III) along with Table 2, the effect of Ag NWs and Au NSs conjunction with rGO-based immunosensors can be seen, respectively; at the same time, their respective calibration curves are depicted within Figure S4 (b) and (c). As showed, the intensity of appeared peaks in plasma samples was increased by a soar in the concentration of the viral antigen. Besides, according to the obtained data, the developed immunosensor based on rGO-EDC/NHS-AB-Au NS exhibits the best detection limit towards identifying SARS-CoV-2's antigen within biological media. In contrast, conjugated immunosensor based on Ag NWs showed the highest intensity compared with other platforms. However, conjugation of Ag NWs with rGO-based immunosensor adversely affects the sensitivity and LOD of the final platform, which is due to the appearance of a sharp peak at the voltage position of 0.12 V arise from Ag NWs, which overshadows the related peak of SARS-CoV-2's antigen (Fig. 4 (d)) and subsequently increase the LOD from 0.0011 fg mL^{-1} to 0.00652 fg mL^{-1} and decline the sensitivity of about 30.51% compared with rGO-NHS/EDC-AB.

Additionally, despite the fact that the conjunction of rGO-NHS/EDC-AB with Au Ns can improve the LOD by about 12.15%, but it can adversely affect the sensitivity and decline it by about 21.04%. A decline in the platform's sensitivity via the addition of either Ag NWs or Au NSs could be due to the occupation of hydrogen-based functional groups via the aforementioned metallic compounds. However, as differences are negligible because of their order (10^{-18}), the LOD is mainly considered an essential detection criterion. Hence, the rGO-based immunosensor in conjunction with Au NSs was selected as the optimum platform for identifying SARS-CoV-2 antigen and surveying the responsible detection mechanism of the proposed immunosensor. The superior catalytic performance of the conjugated immunosensor with Au NSs could be attributed to the final platform's boosted electrical conductivity and electrocatalytic performance upon introducing Au NSs to the nano-immunocomplex. More importantly, no prominent peak was traced at the active surface of the modified GCE with rGO-EDC-NHS-AB-Au NS in the absence of SARS-CoV-2's antigen, which shows the excellent specificity of the immunosensor toward SARS-CoV-2. The main parameter in such behaviour is related to the presence of rGO as an efficient substrate by providing a higher specific surface area compared with other carbonaceous nanomaterials.

What is more, to assess the applicability of the developed sensor for real applications, the influence of some typical electroactive interfering compounds was appraised in the human blood plasma sample on the current response of SARS-CoV-2's antigen with an initial concentration of 0.016 fg mL^{-1} through the addition of 0.5 mM interfering biomolecules to the electrolyte, e.g., glucose, fructose, sucrose, lactose, ascorbic acid (AA), K^+, Zn^{2+} and two different types of influenza viruses, i.e., H_1N_1 and H_3N_2. As depicted within Fig. 4 (e), achieved outcomes did not reveal any notable discrepancy in the I_p of the SARS-CoV-2 antigen highlighting the superior capability of the rGO-based immunosensor toward accurate recognition of target viruses even in the presence of interfering compounds at high loadings. However, the peak current of ascorbic acid appeared at a voltage position of 0.2 V, which is not in the desired potential window of the SARS-CoV-2 antigen. Moreover, the existence of influenza viruses did not affect the sensor's response, which furtherly highlights the specific response of the immunosensor to the antigen of SARS-CoV-2.

After selecting a conjugated rGO-based immunosensor with Au NSs as the optimum immunosensor for precise and specific identification of SARS-CoV-2 antigen in natural biological fluids, the CV and DPV analyses were used to examine the detection mechanism of antigen via antibody through immunoreaction process. The CV method is a well-known diagnostic approach for characterizing target compounds and appraisement of responsible electrochemical mechanisms of chemical processes. Accordingly, the possible mechanism for adsorption of viral antigen on the modified electrode surface was initially investigated by CV analyses. To check the governing electrocatalytic mechanism of the proposed technique, the influence of potential scan rate on the output response of the CV technique was precisely assessed. As demonstrated in Figure S5 (a), upon further soar in the scan rate from 0.03 to 0.5 V s^{-1}, a very weak output current signal was traced; the respective calibration curve of this plot can be seen in Figure S6. Correspondingly, variation of the respective currents of anodic peaks through a further increase in the scan rate revealed that the process is controlled via the surface-confined reaction and adsorptive direct electron transfer process on the active surface of the modified electrode.

What is more, owing to the low sensitivity and/or resolution of the CV approach for assessing the electrochemical mechanism of immune interaction between antibody and target antigen, the DPV method as a more sensitive voltammetric approach was used owing to its far greater resolution. Thereby, more proper diagnostic criteria were achieved using the DPV assay to recognize various mechanisms occurring on the active surface of the coated electrode with an immunosensor. In this matter, either positive or negative potential is applied to the electrode via DPV assay, and the respective signal was isolated to check the detection mechanism. As depicts within Figure S5 (b), the outcome of

Table 2
Quantitative analysis of figures of merit of rGO-based immunosensors with either Ag NWs or Au NSs as amplifying agents (n=3).

Electrode	Linear range ($fg.mL^{-1}$)	LOD ($fg.mL^{-1}$)	Linear Regression Equation	Sensitivity ($\mu A.(fg/mL)^{-1}.cm^{-2}$)	R^2
rGO-NHS/EDC-AB	0.0013–0.028	0.0011	ΔJ ($\mu A.cm^{-2}$) = 14.168±0.3 C($fg.mL^{-1}$)+ 0.0366±0.001	59.28	0.9894
rGO-NHS/EDC-AB-Ag NWs	0.0076–0.036	0.0065	ΔJ ($\mu A.cm^{-2}$)= 9.7706±0.08 C ($fg.mL^{-1}$)+ 0.0473±0.004	19.05	0.9931
rGO-NHS/EDC-AB-Au NSs	0.0012–0.025	0.0010	ΔJ ($\mu A.cm^{-2}$)= 10.755±0.1 C ($fg.mL^{-1}$)+ 0.0104±0.003	17.49	0.9957

the DPV process in PBS solution with pH 7.4 describes low peak segregation somewhat about ~36 mV between the cathodic and anodic peaks, which showed ip_a/ip_c of 2.316, indicating the specific immune reaction between the monoclonal IgG antibody against S1 glycoprotein of SARS-CoV-2 and its target antigen. These outcomes are in perfect accord with the chemical-electrochemical C_iE_r mechanism.

3. Conclusion

The widespread of viral infectious diseases originated from airborne viruses, e.g., SARS-CoV-2, raised the global concern for developing effective approaches capable of specific, sensitive, and rapid detection of target pathogens for prompt identification of infected people. For this aim, carbonaceous immunosensors proved to be ideal alternatives instead of common approaches owing to their superior specificity, inherited from an immunoreaction between the mounted antibody and the target antigen. In the current study, electrocatalytic performance, NHS/EDC activation rate, and antibody loading efficiency of various types of 1D and 2D carbonaceous nanomaterials, e.g., MWCNTs and graphene derivatives, were assessed to find the most proper configuration for the development of effective immunosensors. Accordingly, the outcome of assessments revealed the superiority of reduced GO over other carbonaceous materials owing to its wider active surface area, higher electrical conductivity, and superior electrocatalytic activity. The rGO-based immunosensor showed antibody loading rate of 6.33×10^{-9} mol cm^{-2} along with LOD/sensitivity of 0.001 fg mL^{-1}/59.28 μA(fg/mL)$^{-1}$.cm^{-2}. What is more, the effect of Au NSs and Ag NWs conjugation with rGO-based immunosensor is also assessed, which showed the potential of Au NSs for improving the LOD of the configuration and the adverse effect of Ag NWs on both sensitivity and LOD of the final platform. The outcome of this study paves the way toward the development of reliable carbonaceous immunosensors with optimized parameters toward rapid detection of ill people and stopping the transfer chain of a pandemic originated from rapid transferable viruses.

Credit for authors statement

Seyyed Alireza Hashemi: Conceptualization, Methodology, Validation, Formal analysis, Investigation, Resources, Data curation, Writing – original draft, Writing – review & editing, Visualization, Project administration. Sonia Bahrani, Conceptualization, Methodology, Validation, Investigation, Data curation, Writing – original draft, Visualization. Seyyed Mojtaba Mousavi, Validation, Formal analysis, Resources, Funding acquisition. Navid Omidifar, Conceptualization, Methodology, Validation, Formal analysis, Resources, Visualization, Funding acquisition. Nader Ghaleh Golab Behbahan, Resources. Mohammad Arjmand, Validation, Formal analysis, Supervision. Seeram Ramakrishna, Validation, Formal analysis, Supervision. Ayrat M. Dimiev, Validation, Formal analysis, Investigation, Data curation. Kamran Bagheri Lankarani, Validation, Formal analysis, Supervision. Mohsen Moghadami, Validation, Formal analysis. Mohammad Firoozsani, Resources, Funding acquisition

Declaration of competing interest

The authors declare that they have no known competing financial interests or personal relationships that could have appeared to influence the work reported in this paper.

Acknowledgment

The supporting information shows the full details of the experimental section and further assessments of fabricated immunosensors. Additionally, all of the performed tests were conducted by considering all of the required standard procedures. The project is performed by considering all of the ethical standards/guidelines and registered in the Shiraz University of Medica Sciences as a part of a project with the ethics code of IR.SUMS.REC.1400.005.

Appendix A. Supplementary data

Supplementary data to this article can be found online at https://doi.org/10.1016/j.talanta.2021.123113.

References

[1] X. Zhu, X. Wang, L. Han, T. Chen, L. Wang, H. Li, S. Li, L. He, X. Fu, S. Chen, Multiplex reverse transcription loop-mediated isothermal amplification combined with nanoparticle-based lateral flow biosensor for the diagnosis of COVID-19, Biosens. Bioelectron. 166 (2020) 112437.
[2] S.M. Mousavi, S.A. Hashemi, N. Parvin, A. Gholami, S. Ramakrishna, N. Omidifar, M. Moghadami, W.-H. Chiang, S. Mazraedoost, Recent biotechnological approaches for treatment of novel COVID-19: from bench to clinical trial, Drug Metabol. Rev. (2020) 1–30.
[3] S.A. Hashemi, S. Bahrani, S.M. Mousavi, N. Omidifar, N.G.G. Behbahan, M. Arjmand, S. Ramakrishna, K.B. Lankarani, M. Moghadami, M. Shokripour, Ultra-precise label-free nanosensor based on integrated graphene with Au nanostars toward direct detection of IgG antibodies of SARS-CoV-2 in blood, J. Electroanal. Chem. (2021) 115341.
[4] S.A. Hashemi, N.G.G. Behbahan, S. Bahrani, S.M. Mousavi, A. Gholami, S. Ramakrishna, M. Firoozsani, M. Moghadami, K.B. Lankarani, N. Omidifar, Ultra-sensitive viral glycoprotein detection NanoSystem toward accurate tracing SARS-CoV-2 in biological/non-biological media, Biosens. Bioelectron. 171 (2021) 112731.
[5] L. Krejcova, P. Michalek, M.M. Rodrigo, Z. Heger, S. Krizkova, M. Vaculovicova, D. Hynek, V. Adam, R. Kizek, Nanoscale virus biosensors: state of the art, Nanobiosensors in Disease Diagnosis 4 (2015) 47–66.
[6] S.A. Hashemi, N.G.G. Behbahan, S. Bahrani, S.M. Mousavi, A. Gholami, S. Ramakrishna, M. Firoozsani, M. Moghadami, K.B. Lankarani, N. Omidifar, Ultra-sensitive viral glycoprotein detection NanoSystem toward accurate tracing SARS-CoV-2 in biological/non-biological media, Biosens. Bioelectron. 171 (2020) 112731.
[7] X.-T. Ma, X.-W. He, W.-Y. Li, Y.-K. Zhang, Epitope molecularly imprinted polymer coated quartz crystal microbalance sensor for the determination of human serum albumin, Sensor. Actuator. B Chem. 246 (2017) 879–886.
[8] F.S. Felix, L. Angnes, Electrochemical immunosensors–a powerful tool for analytical applications, Biosens. Bioelectron. 102 (2018) 470–478.
[9] C. Kokkinos, A. Economou, M.I. Prodromidis, Electrochemical immunosensors: critical survey of different architectures and transduction strategies, Trac. Trends Anal. Chem. 79 (2016) 88–105.
[10] J. Lin, H. Ju, Electrochemical and chemiluminescent immunosensors for tumor markers, Biosens. Bioelectron. 20 (8) (2005) 1461–1470.
[11] J.-Z. Tsai, C.-J. Chen, K. Settu, Y.-F. Lin, C.-L. Chen, J.-T. Liu, Screen-printed carbon electrode-based electrochemical immunosensor for rapid detection of microalbuminuria, Biosens. Bioelectron. 77 (2016) 1175–1182.
[12] A.M. Dimiev, S. Eigler, Graphene Oxide: Fundamentals and Applications, wiley2016.
[13] A. Khannanov, B. Gareev, G. Batalin, L.M. Amirova, A.M. Dimiev, Counterion concentration profiles at the graphene oxide/water interface, Langmuir 35 (41) (2019) 13469–13479.
[14] L. Fritea, F. Bănică, T.O. Costea, L. Moldovan, C. Iovan, S. Cavalu, A gold nanoparticles-Graphene based electrochemical sensor for sensitive determination of nitrazepam, J. Electroanal. Chem. 830 (2018) 63–71.
[15] S.A. Hashemi, S.M. Mousavi, S. Bahrani, S. Ramakrishna, Integrated polyaniline with graphene oxide-iron tungsten nitride nanoflakes as ultrasensitive electrochemical sensor for precise detection of 4-nitrophenol within aquatic media, J. Electroanal. Chem. 873 (2020) 114406.
[16] B.S. Zadeh, H. Esmaeili, R. Foroutan, S.M. Mousavi, S.A. Hashemi, Removal of Cd (II) from aqueous solution using eucalyptus sawdust as a bio-adsorbent: kinetic and equilibrium studies, J Environ Treat Tech 8 (1) (2020) 112–118.
[17] S.M. Mousavi, F.W. Low, S.A. Hashemi, N.A. Samsudin, M. Shakeri, Y. Yusoff, M. Rahsepar, C.W. Lai, A. Babapoor, S. Soroshnia, Development of hydrophobic reduced graphene oxide as a new efficient approach for photochemotherapy, RSC Adv. 10 (22) (2020) 12851–12863.
[18] K. Sheng, W. Liu, L. Xu, Y. Jiang, X. Zhang, B. Dong, G. Lu, H. Song, An ultra-sensitive label-free immunosensor toward alpha-fetoprotein detection based on three–dimensional ordered IrOx inverse opals, Sensor. Actuator. B Chem. 254 (2018) 660–668.
[19] Y. Niu, T. Yang, S. Ma, F. Peng, M. Yi, M. Wan, C. Mao, J. Shen, Label-free immunosensor based on hyperbranched polyester for specific detection of α-fetoprotein, Biosens. Bioelectron. 92 (2017) 1–7.
[20] C. Liu, J. Dong, G.I. Waterhouse, Z. Cheng, S. Ai, Electrochemical immunosensor with nanocellulose-Au composite assisted multiple signal amplification for detection of avian leukosis virus subgroup, J. Biosens. Bioelectron. 101 (2018) 110–115.
[21] L.A. Layqah, S. Eissa, An electrochemical immunosensor for the corona virus associated with the Middle East respiratory syndrome using an array of gold nanoparticle-modified carbon electrodes, Microchimica Acta 186 (4) (2019) 1–10.

[22] A. Sharma, A. Kaushal, S. Kulshrestha, A Nano-Au/C-MWCNT based label free amperometric immunosensor for the detection of capsicum chlorosis virus in bell pepper, Arch. Virol. 162 (7) (2017) 2047–2052.
[23] S. Alwarappan, K. Cissell, S. Dixit, C.-Z. Li, S. Mohapatra, Chitosan-modified graphene electrodes for DNA mutation analysis, J. Electroanal. Chem. 686 (2012) 69–72.
[24] S. Alwarappan, S. Prabhulkar, A. Durygin, C.-Z. Li, The effect of electrochemical pretreatment on the sensing performance of single walled carbon nanotubes, J. Nanosci. Nanotechnol. 9 (5) (2009) 2991–2996.
[25] G. Seo, G. Lee, M.J. Kim, S.-H. Baek, M. Choi, K.B. Ku, C.-S. Lee, S. Jun, D. Park, H. G. Kim, Rapid detection of COVID-19 causative virus (SARS-CoV-2) in human nasopharyngeal swab specimens using field-effect transistor-based biosensor, ACS Nano 14 (4) (2020) 5135–5142.
[26] R.M. Torrente-Rodríguez, H. Lukas, J. Tu, J. Min, Y. Yang, C. Xu, H.B. Rossiter, W. Gao, SARS-CoV-2 RapidPlex: a graphene-based multiplexed telemedicine platform for rapid and low-cost COVID-19 diagnosis and monitoring, Matter 3 (2020) 1981–1998.
[27] B.R. Smith, S.S. Gambhir, Nanomaterials for in vivo imaging, Chem. Rev. 117 (3) (2017) 901–986.
[28] V. Stanković, S. Đurđić, M. Ognjanović, B. Antić, K. Kalcher, J. Mutić, D. M. Stanković, Anti-human albumin monoclonal antibody immobilized on EDC-NHS functionalized carboxylic graphene/AuNPs composite as promising electrochemical HSA immunosensor, J. Electroanal. Chem. 860 (2020) 113928.
[29] L. Fabiani, M. Saroglia, G. Galatà, R. De Santis, S. Fillo, V. Luca, G. Faggioni, N. D'Amore, E. Regalbuto, P. Salvatori, Magnetic beads combined with carbon black-based screen-printed electrodes for COVID-19: a reliable and miniaturized electrochemical immunosensor for SARS-CoV-2 detection in saliva, Biosens. Bioelectron. 171 (2021) 112686.
[30] S. Mahari, A. Roberts, D. Shahdeo, S. Gandhi, eCovSens-ultrasensitive novel in-house built printed circuit board based electrochemical device for rapid detection of nCovid-19 antigen, a spike protein domain 1 of SARS-CoV-2, BioRxiv (2020).
[31] H. Zhao, F. Liu, W. Xie, T.-C. Zhou, J. OuYang, L. Jin, H. Li, C.-Y. Zhao, L. Zhang, J. Wei, Ultrasensitive supersandwich-type electrochemical sensor for SARS-CoV-2 from the infected COVID-19 patients using a smartphone, Sensor. Actuator. B Chem. 327 (2021) 128899.
[32] S.A. Hashemi, S. Bahrani, S.M. Mousavi, N. Omidifar, M. Arjmand, N.G. G. Behbahan, S. Ramakrishna, K.B. Lankarani, M. Moghadami, M. Firoozsani, Ultrasensitive Biomolecule-Less Nanosensor Based on β-Cyclodextrin/Quinoline Decorated Graphene Oxide toward Prompt and Differentiable Detection of Corona and Influenza Viruses, Advanced Materials Technologies, 2021, p. 2100341.
[33] S. Bahrani, Z. Razmi, M. Ghaedi, A. Asfaram, H. Javadian, Ultrasound-accelerated synthesis of gold nanoparticles modified choline chloride functionalized graphene oxide as a novel sensitive bioelectrochemical sensor: optimized meloxicam detection using CCD-RSM design and application for human plasma sample, Ultrason. Sonochem. 42 (2018) 776–786.
[34] R. KarimiShervedani, S. Bahrani, M. Samiei Foroushani, F. Momenbeik, Selective detection of dopamine in the presence of ascorbic and uric acids through its covalent immobilization on gold mercaptopropionic acid self -assembledMonolayer, Electroanalysis 29 (1) (2017) 272–279.
[35] J. Bard Allen, R. Faulkner Larry, Electrochemical Methods: Fundamentals and Applications, Wiley, New York, 2001.
[36] S.A. Hashemi, S.M. Mousavi, S. Bahrani, S. Ramakrishna, A. Babapoor, W. H. Chiang, Coupled graphene oxide with hybrid metallic nanoparticles as potential electrochemical biosensors for precise detection of ascorbic acid within blood, Anal. Chim. Acta 1107 (2020) 183–192.